Jakub WIERCIAK
Robert MAKOWSKI

STEPPING MOTOR DRIVE SYSTEM REPLACING AC ELECTRIC SERVO DRIVE IN A PROCESSING DEVICE

ABSTRACT *As a result of dynamic development that takes place in the field of controlling AC motors, designers of machines and various devices usually apply servo drives with induction or synchronic motors, relying both on their remarkable operational characteristics as well as their long life. However, advanced electronic systems and sophisticated software, necessary for obtaining such characteristics, are quite expensive. The authors present in the paper an example of an actuating system for a processing device powered by AC servo drive. As proved by the model studies that have been carried out, the servo drive can be replaced with a stepping motor that is few times less expensive, and at the same time meets all the requirements related to its operation.*

Keywords: *electrical drives, stepping motors, servo drives.*

1. INTRODUCTION

AC servo drives are commonly applied in contemporary processing devices to realize complex motion functions [2, 4]. They constitute relatively costly part of these machines, yet their remarkable dynamic characteristics are often

Jakub WIERCIAK, Ph.D. Eng., Robert MAKOWSKI, M.Sc. Eng.
e-mail: j.wierciak@mchtr.pw.edu.pl, owsikkk@wp.pl

Warsaw University of Technology,
Institute of Micromechanics and Photonics,
ul. Św. A. Boboli 8, 02-525 Warszawa

PROCEEDINGS OF ELECTROTECHNICAL INSTITUTE, Issue 253, 2011

a sufficient reason to use them. However, there are some cases when designers use servo drives almost habitually, even when their application is not justified by the technical requirements. In such cases, while looking for savings, there are undertaken works aimed to replace servo drives with their cheaper substitutes.

2. DESCRIPTION OF THE ANALYZED DRIVE SYSTEM

In the exemplary processing device, used for transporting and gravitational unloading of containers with semi products, there are two similar drive systems *A* and *B* (Fig. 1), which power the mechanisms of linear motion based on a flexible connector drive with synchronous belt *SYNCHROFLEX 16T10* [14]. During the duty cycle, carriage *A* receives the container from a feeding unit and during its partial unloading moves by 760 mm in total. Then, carriage *B* takes the container and finishes its unloading by moving within a range of 520 mm.

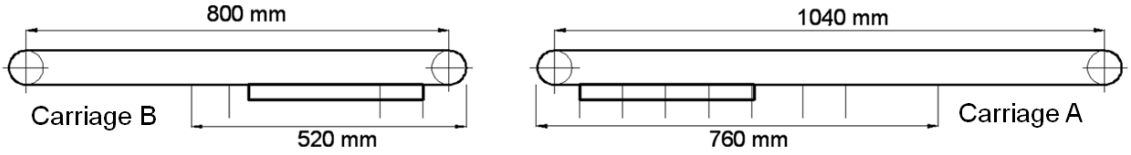

Fig. 1. Ranges of motion of *A* and *B* carriages

The drives are built as closed loop systems with automatic control. A block diagram of the carriage unit is presented in Figure 2. The drive employs AC synchronous motor *SIEMENS 1FK7032-5AK71-1* [12] integrated with a rotation-to-pulse transducer. Additionally, the motor has a built-in power-off brake. When the supply of the motor is off, the brake prevents from a rotation of the shaft and thus from an incidental displacement of the carriage. The torque is transmitted from the motor to the mechanism by a planetary reduction gear *Alpha SP+060* [10] with a ratio of i_p = 10. The carriages move within rolling guides *Bosch Rexroth SNS R1605*. The *PLC* controller *SIMATIC S7-300* [11] used in the machine is at present very popular and thus is often applied in the industry.

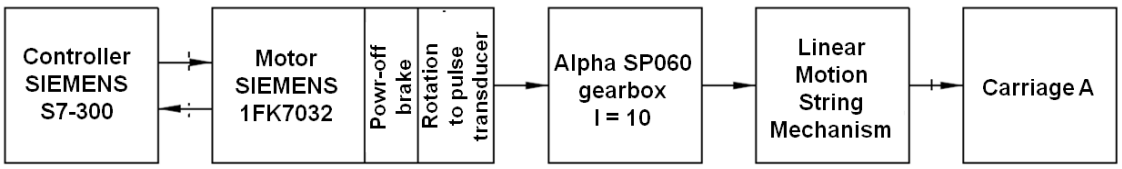

Fig. 2. Block diagram of the drive unit of carriage *A*

Approximate costs of building the drive units of both carriages of the machine for unloading the containers, calculated as a sum of the prices of all their commercial components, are of ca. $ 5,300.

3. REQUIREMENTS REGARDING AN ALTERNATIVE DRIVE

Drives of carriages *A* and *B* operate in a synchronic mode. In order to obtain a high efficiency of the performed operations, when carriage *B* unloads the last two cells of the container, carriage *A* receives a successive full container, and following the previous one, unloads its six cells. The current efficiency of the machine has been accepted as a basic assumption regarding new drives. This means, that besides realization of the linear motions within respective ranges: *carriage A* – 760 mm, *carriage B* – 520 mm, the driving units must ensure positioning of the containers above a chute-type channel in intervals s_{ges} = 81.5 mm, corresponding to the pitch of the container cells (Fig. 3), within time *t* no longer than 0.3 s and with accuracy no lower than 0.5 mm. The drives should also ensure stopping of the carriages at locations corresponding to the final positions and spots where the full containers are received, and the empty ones are deposited.

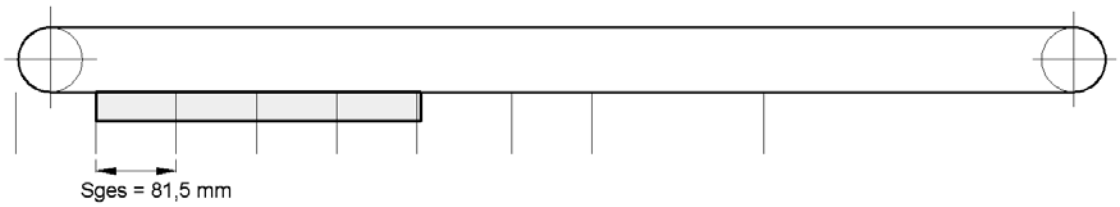

Fig. 3. Displacement s_{ges} of the carriage corresponding to a change of the unloaded cell

Additional requirements concern operation conditions of the drives, especially the range of the ambient temperature from +18ºC to +40°C, as well as the economics of the undertaking. New drives must be capable of integration with the control system *Siemens SIMATIC S7-300*, and the scope of foreseen modifications of the present design should be as small as possible.

4. THE PROPOSED SOLUTION

As an alternative to the present solutions, the authors proposed an open loop control system powered by an electric stepping motor. Structure of this

drive is presented in Figure 4. The controller of the system receives information on a current position of the rotor of the driving motor, since each pulse timing the motor is counted and it theoretically corresponds to a rotation of the rotor by a known angular displacement equal to one step. In order to verify if such drive system is capable of meeting the functional requirements set for the drives of the carriages, a model studies were carried out.

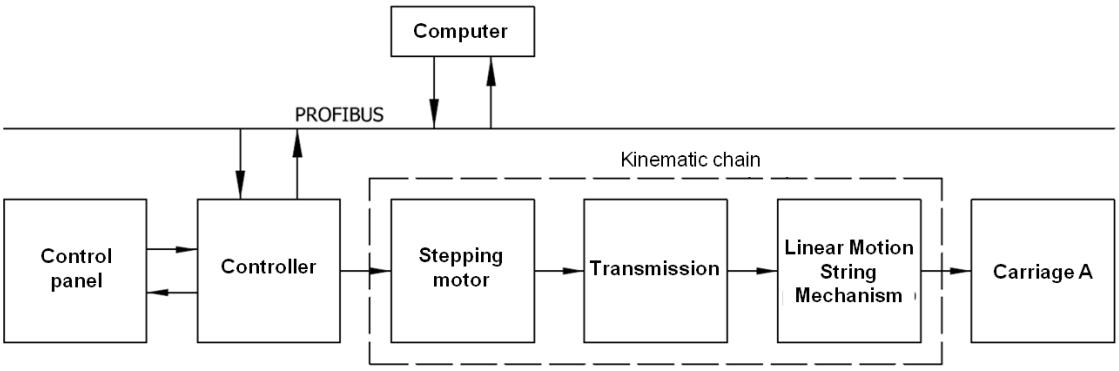

Fig. 4. Structure of an open loop control system for a stepping motor

5. MATHEMATIC MODEL OF THE SYSTEM

5.1. Model of the mechanism

Model of the mechanism of motion conversion based on a flexible connector drive was created as a set of loads of the drive unit. In the case of units where high precision and synchronization is required, initial tension of the toothed belts is introduced. The higher the transmitted powers and velocities, proportionally the higher tensions and stress in the belt, but at the same time the smaller extension of the belts during motion and the lower inaccuracies of positioning the system [6]. A scheme illustrating loads of the mechanism converting rotary motion into linear one is presented in Figure 5. It regards masses, forces and the mass moment of inertia necessary for displacing the buffer container at the required velocities.

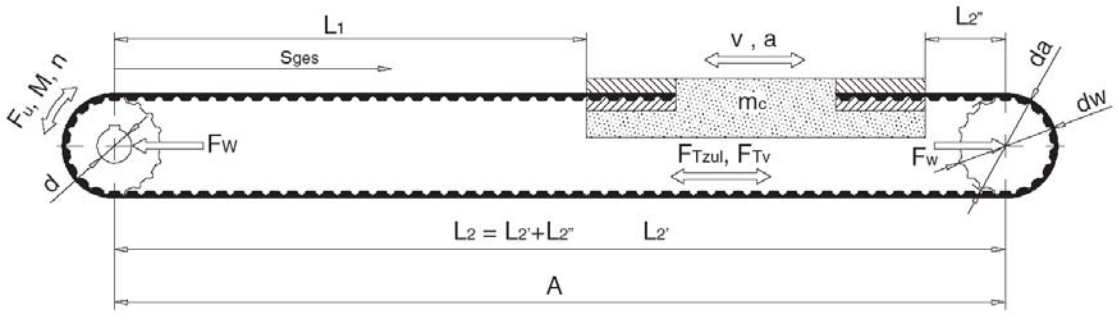

Fig. 5. Scheme of the carriage mechanism used for computing the loads [14]:
a – linear acceleration of the carriage, d_a – tip circle diameter of the toothed wheel, d_w - pitch diameter, d - diameter of the output shaft of the planetary gear, F_u – effective force, F_w – force acting upon the shaft of the wheel, F_{Tzul} – permissible tension of the belt, F_{TV} – force of the initial tension of the belt, A – distance between the axes of the flexible connector drive, L_1 – length of the tensed part of the belt, L_2 – length of the loose part of the belt, M – torque at the driving wheel, m_c – displaced mass, n – rotational speed of the toothed wheel, s_{ges} – linear displacement of the carriage, v – velocity of the uniform motion

Results of the computations, important with regard to selection of the drive and modeling the system, are listed in Table 1.

TABLE 1
Selected features of the mechanism

Effective force	F_U = 240 N
Mass moment of inertia of the accelerated masses at the output shaft of the gear	J_{mech} = 0.013 kgm^2
Maximal acceleration of the carriage	a_b = 18 m/s^2
Maximal deceleration of the carriage	a_v = 18 m/s^2
Maximal linear velocity of the carriage	v = 0.320 m/s

5.2. Model of the gear

Because of the accepted assumption related to a possibly smallest interference in the existing design of the system, at the stage of initial considerations, the existing planetary gear *Alpha SP+060* installed in the system, was taken into considerations. One carried out a classical reduction of the loads and velocities occurring in the motion conversion mechanism with accordance to the following formulas,

$$M_l = \frac{M_{mech}}{\eta_p \quad i_p} \tag{1}$$

$$J_l = \frac{J_{mech}}{i_p^2} \tag{2}$$

$$\omega_{mech} = \frac{\omega}{i_p}, \tag{3}$$

where:

i_p – ratio of the gear,
J_l – mass moment of inertia reduced to the motor shaft,
J_{mech} – mass moment of inertia of the driven members of the mechanism,
M_l – torque reduced to the motor shaft,
M_{mech} – load torque introduced by the mechanism,
η_p – efficiency of the gear,
ω – angular velocity of the motor shaft,
ω_{mech} – angular velocity of the output shaft of the gear.

In the simulation program the following catalog parameters of the planetary gear *Alpha SP+060* were accepted: i_p = 10, η_p = 97%.

5.3. Model of the stepper motor

Using results of the computations regarding the loads, a stepping motor had been initially selected for the analyzed drive. On the basis of the value of the maximal torque and the mechanical characteristic, a hybrid stepping motor *FULLING FL86STH118-6004A* was selected. The related catalog data are listed in Table 2.

TABLE 2
Selected catalog data of the *FULLING FL86STH118-6004A* motor

Maximal torque	M_m = 8.53 N·m
Mass moment of inertia of the rotor	J_m = 0.27 10^{-3} kg·m^2
Number of teeth of the rotor	Z_r = 50
Step	Θ = 0.03141593 rad (1.8º)
Maximal pull-in frequency of the full-step operation	f_{gmax} = 3000 Hz (900 rpm)

Because of the available data, it was decided to use in the simulation experiments so-called „idealized” model of the stepping motor [5]. The model

employs an approximation of the energy conversion with a sinusoidal relation between the torque and angle δ representing deviation between magnetic fields of the rotor and the stator, as well as the coefficient of internal damping D_m. For a hybrid stepping motor, the model can be expressed in a form of an equation of rotational motion

$$\left(J_m + J_l\right)\frac{\mathrm{d}^2\gamma}{\mathrm{d}t^2} + D_m\frac{\mathrm{d}\gamma}{\mathrm{d}t} + \left(M_{mf} + M_{lf}\right)\mathrm{sgn}\left\{\frac{\mathrm{d}\gamma}{\mathrm{d}t}\right\} + M_l = M_e \ , \tag{4}$$

where the electromagnetic torque M_e of the motor is determined as

$$M_e = -M_{\mathrm{m}}\sin\left(\delta\right), \tag{5}$$

and angle δ,

$$\delta = Z_{\mathrm{r}}\left[\gamma - \gamma_u\left(t\right)\right]. \tag{6}$$

The remaining denotations occurring in the equations are:

D_m – coefficient of electromagnetic damping of the motor,
J_m – mass moment of inertia of the rotor,
M_{mf} – internal friction torque in the motor,
M_m – maximal static torque of the motor,
Z_r – teeth number of the rotor,
γ – rotation angle of the rotor,
γ_u – instantaneous position of stable equilibrium of the rotor,
J_l, M_{lf}, M_l – mechanic loads reduced to the motor shaft.

Numerical data for the model were taken from a catalog, and the remaining data were accepted on the basis of experiences that had been gained previously [9]. Especially, it was accepted that D_m = 0.03 N·m/rad/s and M_{mf} = 0.03 N·m. Values of the external loads resulted from the preceding calculations.

5.4. Model of the control system

In the case of the „idealized" model of the stepping motor, the control signal takes a form of successive positions γ_u of the stable equilibrium of the rotor of unloaded motor

$$\gamma_u(t) = \Theta \mathrm{E}\left[1 + u_f(t)\right], \tag{7}$$

where:

E – „entier" function – i.e. integral part of the bracketed value,

Θ – step angle of the motor, and the quantized function $u_f(t)$ is an integral of the required function of the motor timing frequency.

$$u_f(t) = \int f(t)\,\mathrm{d}t\,. \tag{8}$$

This way of generating the control signal results from reasoning, whose essence is illustrated in Figure 6.

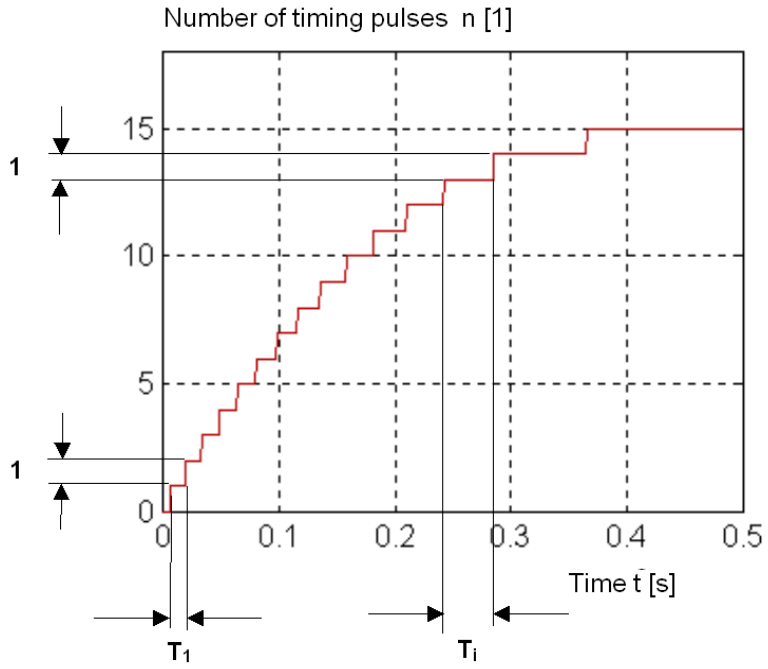

Fig. 6. Principle of generating timing pulses (decreasing timing frequency): T_1 – timing period of the first pulse, T_i – timing period of the i-th pulse

Course of the input signal is transformed into a stepped curve by the quantizing system. Each pulse has the same height equal to 1, yet its length T_i depends on the instantaneous timing frequency

$$T_i = \frac{1}{f(t)}\,. \tag{9}$$

Therefore, derivative of the quantized function can be expressed as

$$\frac{\mathrm{d}u_f(t)}{\mathrm{d}t} = \frac{1}{T_i} = f(t), \tag{10}$$

and hence results equation (8) that has been already presented.

Model of the control system was created in such a way as to allow not only velocity profiles, typical for positioning systems: triangular and trapezoidal (Fig. 7a and 7b), to be easily realized, but also their modifications, which can be introduced in the case of stepping motors, starting at a non-zero frequency f_{start} (Fig. 7c and 7d). Accelerating and decelerating the motor according to nonlinear relations [1], which make it possible to make the most of its characteristics, were not regarded in the modeling in order to simplify the studies.

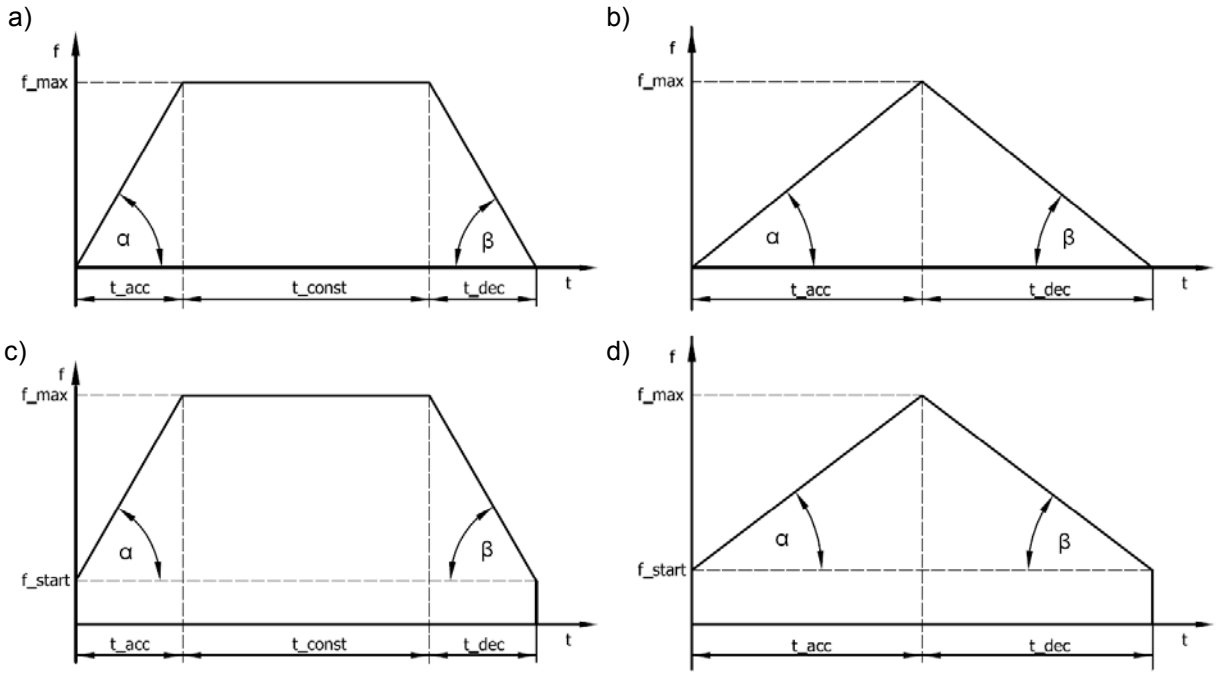

Fig. 7. Frequency profiles generated by the control system:
a) trapezoidal profile, b) triangular profile, c) trapezoidal profile with starting frequency $f_{start} \neq 0$, d) triangular profile with starting frequency $f_{start} \neq 0$; t_acc – acceleration time, t_dec – deceleration time, t_const – time of operation at a constant speed

The simulation model of the whole analyzed actuating system was created in *Matlab-Simulink* language by combining the described above models of particular subunits.

6. SIMULATION STUDIES

6.1. Studies on the original drive system

A series of simulation experiments of the modeled drive system was carried out. Once motion parameters had been set, linear displacement of the carriage was recorded. First simulation experiments were carried out for a triangular frequency course at the following parameters: t_{acc} = 0.15 s, t_{dec} = 0.15 s, t_{const} = 0 s, f_{max} = 3000 Hz, f_{start} = 0 Hz or f_{start} = 580 Hz and the time of simulation limited to t = 0.3 s.

The starting frequency f_{start} was selected on the basis of the pull-in characteristic of the motor [7, 8], which was determined by means of simulation since it was not included in the related catalog data provided by the manufacturer. Course of this characteristic is presented in Figure 8.

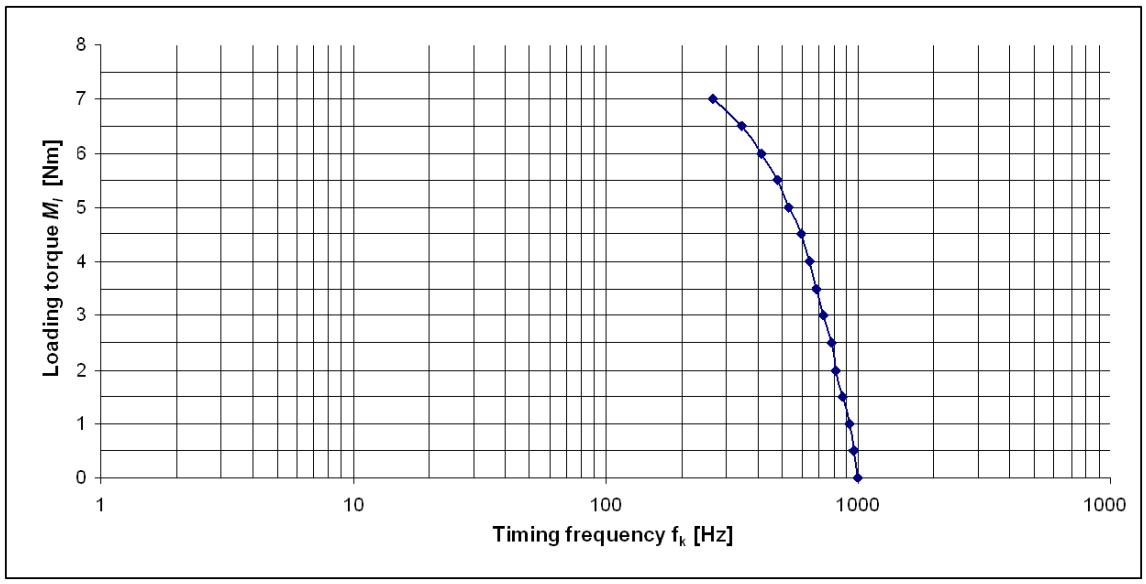

Fig. 8. Pull-in characteristic of *FULLING FL86STH118-6004A* motor determined by means of simulation at the mass moment of inertia equal to the mass moment of inertia of the rotor (J_m = 0.27 10^{-3} kg·m^2)

As frequency f_{max}, one accepted the maximal pull-in frequency of the selected motor equal to 3000 Hz.

The successive studies were carried out using a trapezoidal profile at the following parameters: t_{acc} = 0.03 s, t_{dec} = 0.02 s, t_{const} = 0.25 s, f_{max} = 3000 Hz, f_{start} = 0 Hz or f_{start} = 580 Hz and simulation time limited to t = 0.3 s.

Results of the simulations are illustrated in Figure 9 in a form of time responses of the system; a) and b) for the triangular profile; c) and d) for the trapezoidal profile. The stepping motor was able to displace the carriage by s = 82.5 mm, meeting thus the basic requirement, at a zero starting frequency only in the case of the trapezoidal profile. Control according to the triangular profile ensured displacement of the carriage only by distance s = 45 mm. Setting the starting frequency for f_{start} = 580 Hz resulted in an increase of the carriage displacement up to s = 54 mm, yet it was still too small anyway. Introduction of a starting frequency and control according to the trapezoidal profile influenced the displacement only a little bit. Within the assumed time t_{ges} = 0.3 s distance s = 84.0 mm was obtained.

6.2. Studies on the drive system with the new gear

Studies on a modified drive system were carried out. A reduction gear having a smaller ratio i = 7 had been selected from the catalog of *Alpha* company. It had overall and assembly dimensions the same as the original gear that had been applied hitherto. Smaller ratio makes it possible to obtain bigger linear displacements of the carriage at the same rotation angle of the rotor. At the same time, the moment of inertia of the load reduced to the motor shaft increased. The proposed changes were introduced to the model. The studies were repeated for parameters of the control signals identical as before, giving up on accelerating the motor from a zero frequency. Results of these simulation studies are presented in Figure 10. Using the triangular velocity profile the carriage displaced by s = 77 mm, so still not long enough to meet the basic functional requirement. However, simulation of controlling the modified system according to the trapezoidal frequency profile yielded positive results. Within time t_{ges} = 0.3 s the carriage was displaced along distance s = 120 mm, so definitely exceeding the required value.

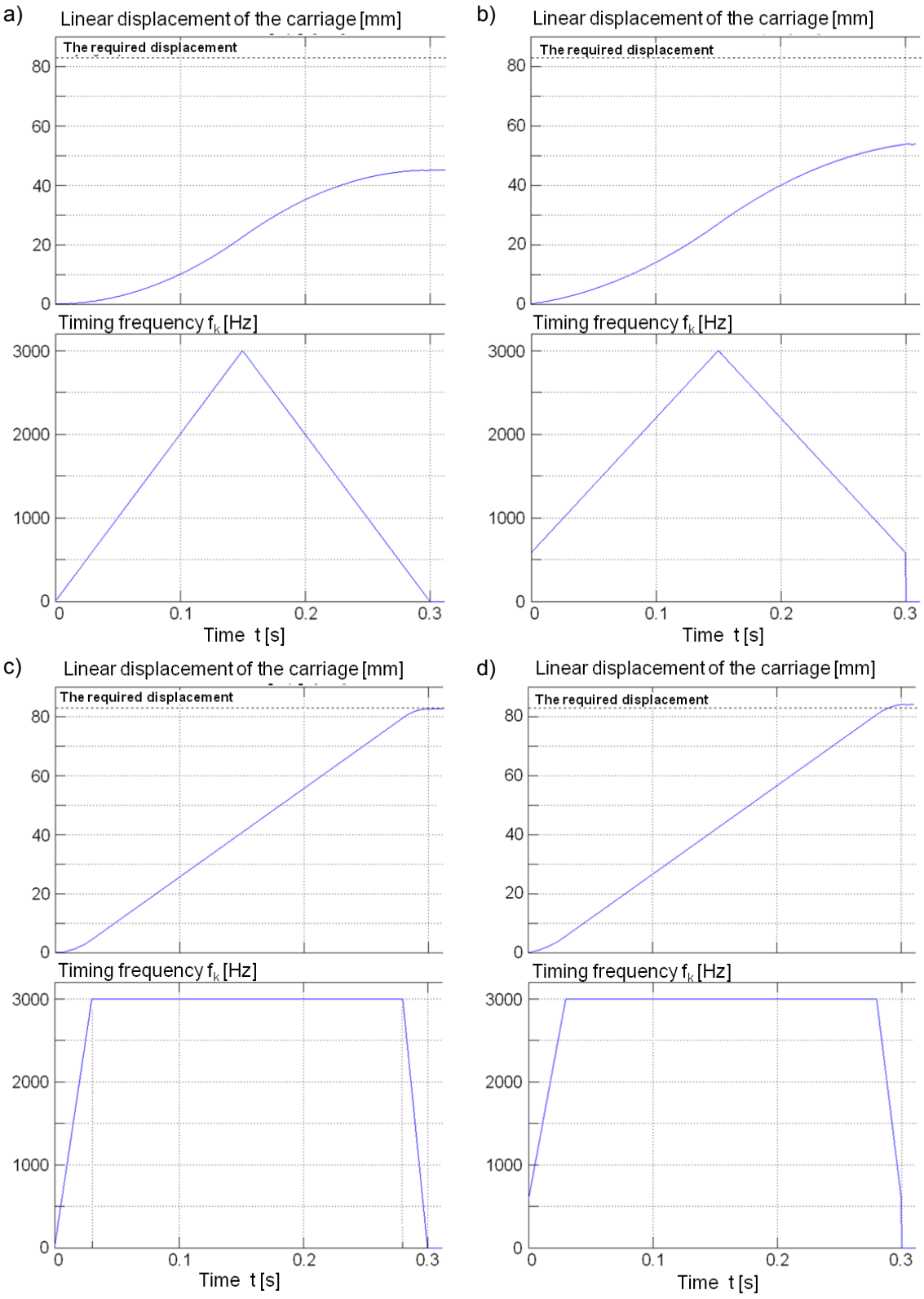

Fig. 9. Courses of the displacement of the carriage for the gear with ratio *i* = 10 at various profiles of the velocity of the driving motor: a) triangle, b) triangle with f_{start} = 580 Hz, c) trapezoidal, d) trapezoidal with f_{start} = 580 Hz

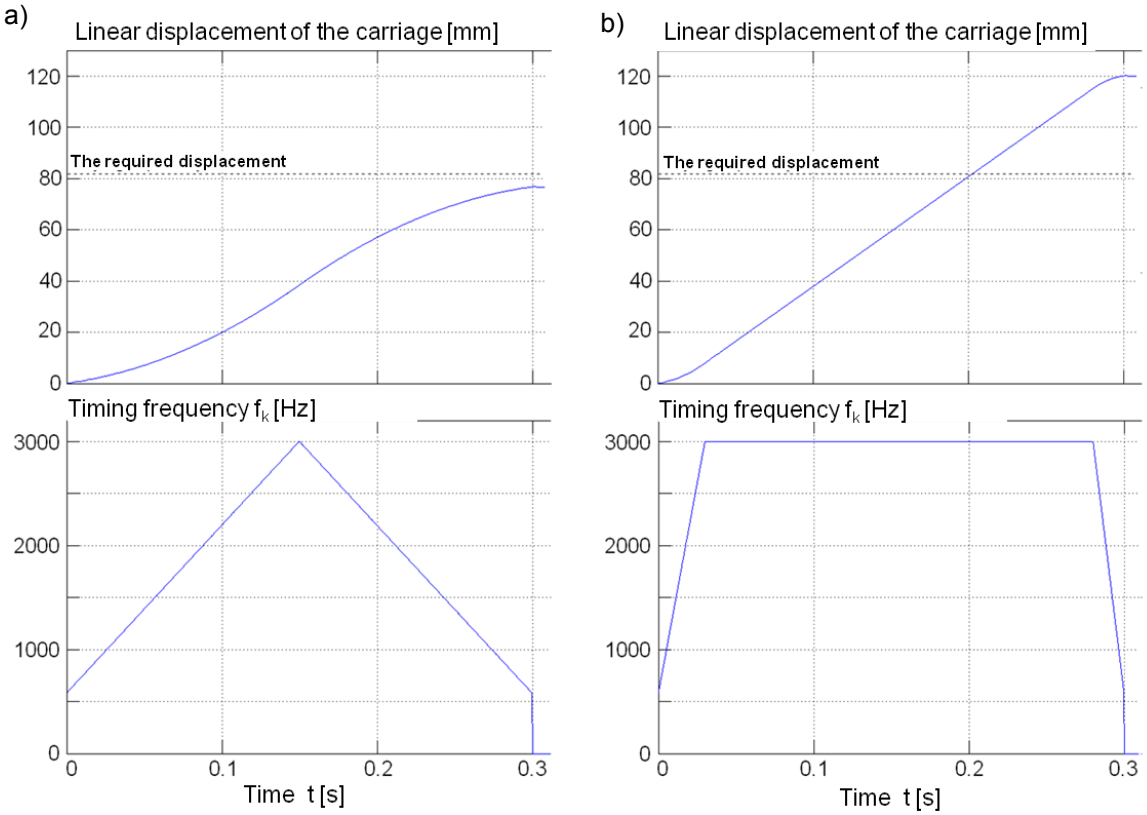

Fig. 10. Courses of the displacement of the carriage for the gear with ratio *i* = 7 at various profiles of the velocity of the driving motor: a) triangle with f_{start} = 580 Hz, b) trapezoidal with f_{start} = 580 Hz

7. SUMMARY AND CONCLUSIONS

The studies that have been carried out proved that it is possible to realize a function of an industrial AC servo drive applied for synchronous displacement of members of a processing device, while using a drive powered by a stepping motor operating in an open loop. The total costs of the elements of the new drives, i.e.: motors, controllers, power suppliers and connection cords slightly exceed $ 880, what is a sum considerably lower compare to the current costs reaching $ 5,300. The proposed solution is capable of meeting the other technical requirements as well, including those related to the positioning accuracy. The obtained resolution of the linear motion of the carriage being of ca. 0.1 mm for a single step of the motor should be high enough to ensure that the currently acceptable error of cell position with respect to the chute-type channel being of ca. 0.3 mm is not exceeded. Additionally, the drives with stepping motors can be controlled by the control system *Siemens SIMATIC S7-300* employed in the device, what was also one of the requirements. The obtained results allow us to formulate conclusions of a more general character.

1. Strategy of squeezing activities related to the products, typical especially for companies characterized by big-lot and mass production, can be also applied in the case of piece production, provided it is related to expensive products, equipped with advanced control systems and costly subunits. In such cases, it pays off to review the existing design and look for savings everywhere it is reasonable. The example presented in the paper proves this thesis.
2. It may be expected that the market of producer goods offers more devices equipped with servo drives that could be replaced with cheaper drives based on stepping motors. The fact that the designers avoid such solutions may result both from their limited knowledge, being accustomed to certain schemes, as well as unwillingness to undertake a risk related to application of subunits they have not used before.

LITERATURE

1. Acarnley P. P.: *Stepping Motors: A guide to modern theory and practice*. IEE. London 2002.
2. Isermann R.: *Mechatronic Systems – Fundamentals*. Springer, 2005.
3. Kenjo T., Sugawara A.: *Stepping Motors and their Microprocessor Controls*. Clarendon Press. Oxford 2003.
4. Kiel E. (Ed.): *Drive solutions. Mechatronics for Production and Logistics*. Springer-Verlag. Berlin 2008.
5. Pochanke A., Wierciak J.: *Trzy modele silnika skokowego hybrydowego*. Proc. of Międzynarodowe XIII Sympozjum „Mikromaszyny i Serwonapędy", Krasiczyn, 15-18.09.2002, vol. II, pp. 389-394 (in Polish).
6. Branowski B. (Ed.): *Podstawy konstrukcji napędów maszyn*. Wydawnictwo Politechniki Poznańskiej. Poznań 2007 (in Polish).
7. Oleksiuk W. (Ed.): *Konstrukcja przyrządów i urządzeń precyzyjnych*. WNT. Warszawa, 1996 (in Polish).
8. Sochocki R.: *Mikromaszyny elektryczne*. OWPW. Warszawa, 1996 (in Polish).
9. Wierciak J., Pochanke A.: *Identyfikacja współczynników modelu hybrydowego silnika skokowego*. Proc. of XII Sympozjum „Modelowanie i Symulacja Systemów Pomiarowych". Krynica 16-20.09.2002, pp. 175-182 (in Polish).
10. *ALPHA*. Products Catalog - Reduction Gears. (www.wamex.com.pl/alpha/Alpha/SP%20Plus_PL.pdf) (in Polish).
11. *SIEMENS*. Products Catalog. (http://www.automatyka.siemens.pl/) (in Polish).
12. *SIEMENS*. Products Catalog. (http://www.preisroboter.de/ergebnis4216714.html).
13. *SIMOTION*. Products Catalog – Controllers (http://www.simotion.pl/) (in Polish).
14. *SYNCHROFLEX*. Products Catalog – Timing Belts (http://www.whm.pl) (in Polish).

Manuscript submitted 09.12.2011

NAPĘD Z SILNIKIEM SKOKOWYM ZAMIAST SERWONAPĘDU W URZĄDZENIU TECHNOLOGICZNYM

Jakub WIERCIAK, Robert MAKOWSKI

STRESZCZENIE *Dynamiczny rozwój, jaki dokonuje się w dziedzinie sterowania silników prądu przemiennego powoduje, że konstruktorzy maszyn i urządzeń chętnie stosują serwonapędy z silnikami indukcyjnymi lub synchronicznymi licząc zarówno na ich znakomite charakterystyki funkcjonalne, jak i dużą trwałość. Zaawansowane układy elektroniczne i wyrafinowane oprogramowanie, które umożliwiają uzyskanie takich charakterystyk są jednak dosyć kosztowne. W artykule przedstawiono przykład układu wykonawczego urządzenia technologicznego, napędzanego przez serwonapęd prądu przemiennego. Przeprowadzono badania modelowe, które wykazały, że serwonapęd ten można zastąpić napędem z silnikiem skokowym, wielokrotnie od niego tańszym, spełniającym przy tym wszystkie wymagania funkcjonalne.*

IEl, Warszawa 2011. Nakład 170 egz. Ark. wyd. 15,22. Ark. druk. 11,25. Pap. off. Kl.III. 80 g.
Oddano do druku w grudniu 2011 r. Druk ukończono w styczniu 2012 r.
Redakcja – Wydawnictwo Instytutu Elektrotechniki
Indeks nr 37656